

RSC Advances



This is an *Accepted Manuscript*, which has been through the Royal Society of Chemistry peer review process and has been accepted for publication.

Accepted Manuscripts are published online shortly after acceptance, before technical editing, formatting and proof reading. Using this free service, authors can make their results available to the community, in citable form, before we publish the edited article. This *Accepted Manuscript* will be replaced by the edited, formatted and paginated article as soon as this is available.

You can find more information about *Accepted Manuscripts* in the [Information for Authors](#).

Please note that technical editing may introduce minor changes to the text and/or graphics, which may alter content. The journal's standard [Terms & Conditions](#) and the [Ethical guidelines](#) still apply. In no event shall the Royal Society of Chemistry be held responsible for any errors or omissions in this *Accepted Manuscript* or any consequences arising from the use of any information it contains.

COMMUNICATION

Correlating *S*-nitrosothiol decomposition and NO release for modified poly(lactic-*co*-glycolic acid) polymer films

Cite this: DOI: 10.1039/x0xx00000x

Received 00th January 2012,
Accepted 00th January 2012

DOI: 10.1039/x0xx00000x

www.rsc.org/

J. M. Joslin,^a B. H. Neufeld,^a and M. M. Reynolds^{a,b}

This study marks the first parallel measurements where *S*-nitrosothiol behaviour is directly correlated to nitric oxide (NO) release for an established polymer system under exposure conditions that are specific to *S*-nitrosothiol decomposition (i.e. heat, light, pH). These methods are intended to be applied to confirm the NO source in any biomaterial system.

Over the past couple of decades, materials with the capability to release nitric oxide (NO) have gained much interest for biomedical applications. In general, the largest limitations of current implanted devices are related to biofouling from persistent infection and thrombus formation, which ultimately lead to device failure. The ability to impart the therapeutic properties of NO (*i.e.*, anti-platelet, prevent thrombosis and infection, promote wound-healing) into a material system would mark an advancement in biomaterials development toward combatting device failure. Many materials have been reported with the capability to release NO at therapeutically relevant levels by directly incorporating NO donors.¹ The two most common NO donors are *N*-diazeniumdiolates² and *S*-nitrosothiols (RSNOs),³ where RSNOs are gaining interest based upon their biological relevance in NO storage and transfer *in vivo*.⁴ As such, many different material platforms, both biostable and biodegradable, have been presented that are based upon the storage and release of NO via RSNO moieties that are covalently bound to polymer backbones. *S*-Nitrosothiol-incorporated materials include fumed silica particles,⁵ polyesters,⁶ polyurethanes,⁷ hydrogels,⁸ dendrimers,⁹ xerogels,^{10,11} and polymer blends.¹²

The ultimate bioapplication of the material involves the delivery of NO, thus the primary analytical method employed to characterize *S*-nitrosated polymers is solely measuring the release of NO. *S*-Nitrosothiols are usually formed via nitrosation of a thiol site, but can also form due to transnitrosation and oxidative processes^{13,14} When considering the complexity associated with nitrosation processes, it is critical to consider that there may be competitive nitrosation processes occurring rather than the exclusive formation of RSNOs. More specifically, the formation of RSNO is achieved via nitrosation of thiol residues within the system, but other nitrosation products can form depending upon the available

functional groups. Common nitrosation conditions include nitrous acid, alkyl nitrites, or exposure to NO under oxygenated conditions.³ For the first two, it is possible that residual inorganic nitrite or alkyl nitrite could remain trapped within the material, which is an issue since nitrites can serve as NO donors under the appropriate reduction conditions, such as the Cu²⁺ conditions commonly employed to reduce RSNOs.¹⁵ For the NO/O₂ nitrosation, the chemistry of NO results in the formation of NO_x species, such as NO₂, N₂O₃, N₂O₄, HNO₂, under oxygenated conditions in the presence of ambient moisture.¹⁶ These intermediate species are of concern due to their involvement in nitrosation processes.¹⁴ Overall, residual nitrosating agent could contribute alternate sources of NO aside from the intended RSNO donors. Other potential NO sources could be due to the possibility that multiple nitroso species can form during the nitrosation process. For example, in earlier work, we demonstrated that *N*-nitrosamines formed competitively with *S*-nitrosothiols for dextran polymers containing both amine and thiol sites.¹⁷ Due to the versatility of nitrosation chemistry,¹⁴ electrophilic nitrosation could occur on any number of nucleophilic sites along the polymer backbone. Therefore, the ability to characterize the RSNO moiety and monitor its decomposition while simultaneously measuring NO will ensure that other nitroso products are not also giving rise to NO.

Overall, due to the versatility of nitrosation chemistry and the wide array of nitrosating agents available, it is necessary to consider potential products that could contribute to NO release aside from the intended RSNO. However, the current approach in the literature is to characterize the material predominantly by NO detection methods, which indicates nothing about the donor behaviour. Polymers exposed to copper ions consistently demonstrate significantly enhanced NO recovery compared to heat or light initiated decomposition. Therefore, many research groups will expose their *S*-nitrosated polymer to copper in order to “completely” reduce the RSNO to yield a total NO recovery. The recovered NO is then directly attributed back to initial RSNO content in a 1:1 molar ratio.^{5,10,18} However, one study attempted to completely decompose *S*-nitrosothiols via copper and was not 100% effective, likely due to Cu²⁺ coordination to thiol sites in the system.¹⁹ Therefore, the introduction of copper to the system may not be representative of initial RSNO content in terms of NO recovery.

Accurate correlation of NO release with specific donors requires that the material be analysed in real time to ensure that the NO is coming from the donor of interest. It is imperative for these systems that the source of NO from the system is due to the decomposition of the RSNO to ensure no alternate sources of NO. If the kinetics of donor decomposition and NO release do not align, this indicates that other physical processes are occurring within the polymer to give rise to NO. Before these materials can be considered for use in biomedical applications, the source of NO must be identified to eliminate the possibility of side reactions occurring, which may result in unintended results once in a biological system.

Herein, a model polymer based upon poly(lactic-*co*-glycolic acid), *S*-nitrosated PLGH-cysteine, was investigated to understand the rate of donor decomposition compared to those of NO release (Figure 1). The synthesis and spectroscopic characterization of the *S*-nitrosated PLGH-cysteine was published by our group previously.²⁰ This system was chosen for these model studies due to its known solubility and stability properties (in 2:1 methanol:dichloromethane) to enable solution-phase UV-vis measurements. Additionally, UV-vis spectroscopic analysis was previously performed to determine the molar extinction coefficient value corresponding to the λ_{max} at 335 nm for the RSNO.²⁰ The polymer was nitrosated in 2:1 methanol:dichloromethane during exposure to *t*-butyl nitrite for 4 h. Thin films of the nitrosated PLGH derivative were prepared by casting the polymer solution onto glass substrates. The films were further analyzed via Sievers 280i nitric oxide analyzers (NOAs, General Electric) and a UV-visible spectrophotometer (Thermo Electron Evolution 300) to monitor the NO release and RSNO behaviour, respectively. Experiments were performed under simulated physiological conditions (phosphate buffered saline soak, pH 7.4, 37 °C) or dry conditions exposed to UV irradiation.

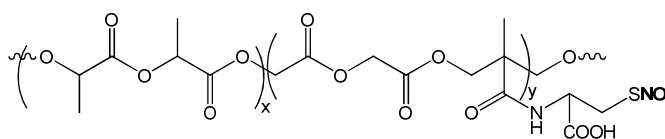


Figure 1. The structure of *S*-nitrosated PLGH-cysteine, where the NO moiety is indicated in bold text.

***S*-Nitrosothiol decomposition via thermal degradation under biological conditions.** To monitor significant changes in the donor decomposition, studies were performed to analyse the RSNO content and NO release as a function of time for films exposed to buffer soak at 37 °C over a 48 h window. The primary mechanisms of *S*-nitrosothiol decomposition under these conditions included pH, temperature, and ambient light. No copper ion was added to solution and the NOA cells and vials employed for this analysis were transparent to ambient UV light. Films for UV-vis analysis were placed into individual vials and purged with N₂. At *t*=0, 4 mL of deoxygenated PBS (37 °C) were injected into each vial, and the films were placed into a water bath for the duration of the analysis interval. Films for RSNO donor studies were analyzed every 12 h, while the films analyzed under NOA underwent a 48 h period on the NOA instrument. For films analyzed via NOA, a film was loaded into a cell, purged with N₂, and at *t*=0, 4 mL of buffer were added. Direct NO measurements were performed via chemiluminescent detection of NO with ozone. Since the NOA setup involved a deoxygenated environment, the films for UV-vis analysis were also deoxygenated via a N₂ purge so that the conditions between the two methods matched. Previous reports have demonstrated that RSNOs undergo accelerated decomposition under aerobic conditions compared to anaerobic conditions due to the presence of N₂O₃,²¹ thus it was additionally important to keep the conditions consistent between methods. The NOA was daily calibrated with 0 and 45 ppm

NO calibrant gases and the sample data was collected real-time with a 5 s collection interval, at a cell pressure of 3.9-4.3 torr, an oxygen supply pressure of 5.1-5.7 psi, and a PMT cooler temperature of -12.0 °C. The released NO was swept into the NOA reaction chamber via a N₂ purge where it was subsequently reacted with O₃ to result in a chemiluminescent response. The produced photon from the reaction of NO and O₃ was detected by a PMT, and subsequently converted to units of ppb. The ppb values were subsequently converted to mol of NO through the use of a calibration constant (mol NO s⁻¹ ppb⁻¹) that is determined through a calibration process involving the reduction of nitrite. All NO values (total mol) were normalized by the mass of the polymer film.

To determine RSNO content within the polymer film at each time point, the polymer sample was dissolved in 2:1 methanol:dichloromethane solvent for subsequent UV-vis analysis. The raw absorbance value at 335 nm was baseline corrected by subtracting out the absorbance value corresponding to the non-nitrosated polymer in solution. Using Beer's Law ($A = \epsilon bc$), the concentration of RSNO (*c*) in units of mol L⁻¹ was determined by dividing the corrected absorbance value (*A*) by the value ϵb , where ϵ was the previously determined molar extinction coefficient value of $882.9 \pm 18.2 \text{ M}^{-1} \text{ cm}^{-1}$,²⁰ and *b* was a fixed pathlength of 1 cm corresponding to the quartz cuvette. The concentration of RSNO in terms of mol L⁻¹ was converted to mmol g⁻¹ using the polymer concentration (3.5 mg mL⁻¹) as a conversion factor. Figure 2 shows the plot of RSNO content and NO release as a function of the 48 h soaking period, while Table 1 shows the values at each time point. It can be seen in Figure 2 that the RSNO content (mmol g⁻¹) over time trace is inverse of the NO release plot. Additionally, the slope corresponding to the 12-48 h data as determined by a linear regression analysis was $1.39 \pm 0.29 \times 10^{-4} \text{ mmol g}^{-1} \text{ h}^{-1}$ for the NO release and $-2.16 \pm 0.60 \times 10^{-4} \text{ mmol g}^{-1} \text{ h}^{-1}$ for RSNO content. At the 95% CL, there is no statistically significant difference between these slopes, indicating that NO release indeed correlates inversely to RSNO decomposition. After the 48 h analysis period, 30% of the initial RSNO content was left.

Table 1. The RSNO content and NO release values as a function of PBS soak time at 37 °C for *S*-nitrosated PLGH-cysteine films. Each data point corresponds to the average and standard deviation of *n*=3.

time (h)	$\mu\text{mol RSNO g}^{-1}$	$\mu\text{mol NO g}^{-1}$
0	37.5 ± 3.1	0.0 ± 0.0
12	20.0 ± 2.2	28.3 ± 0.1
24	15.8 ± 0.9	31.5 ± 0.3
36	16.2 ± 3.6	32.4 ± 0.4
48	11.2 ± 0.4	33.6 ± 0.5

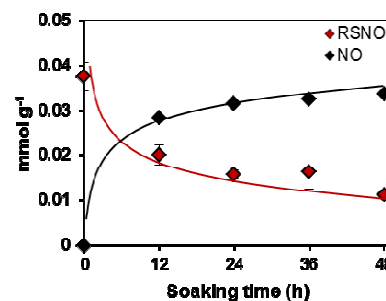


Figure 2. The RSNO decomposition (red) and NO release (black) profiles over time for *S*-nitrosated PLGH-cysteine films exposed to a 37 °C deoxygenated PBS soak over 48 h. Each data point corresponds to the average and standard deviation of *n*=3.

S-Nitrosothiol decomposition under dry, UV-triggered conditions. Additionally, we considered RSNO decomposition and NO release under exposure to UV light. Since UV conditions trigger RSNO decomposition,²² this marks an alternate NO delivery pathway. The films were individually loaded into an NOA cell and exposed to a high intensity UV lamp (365 nm) for 10, 20 or 30 min. After this analysis period, films were collected for solution-phase UV-vis analysis. Control, non-nitrosated films were also exposed to UV light and showed no changes in the UV-vis spectrum. The mmol RSNO g⁻¹ values were determined as described for the PBS soaked films at 37 °C. Figure 3 shows the NO release and RSNO content as a function of UV exposure time, while Table 2 shows the values at each time point.

The slopes corresponding to NO release and RSNO content in Figure 3 were $1.14 \pm 0.11 \times 10^{-3}$ mmol g⁻¹ h⁻¹ and $-1.11 \pm 0.12 \times 10^{-3}$ mmol g⁻¹ h⁻¹, respectively, as determined by a linear regression analysis. At the 95% CL, there is no statistically significant difference between these slopes, indicating that, as for the case of the films soaked in PBS, the UV-initiated RSNO decomposition is directly giving rise to the detected NO. This correlation can be further seen because the total RSNO that decomposed over the 30 min period was 0.034 ± 0.025 mmol g⁻¹, while the total NO that was released was 0.033 ± 0.006 mmol g⁻¹. After the 30 min analysis period, 75% of the initial RSNO remained.

Table 2. The RSNO content and NO release values are shown as a function of UV exposure time for *S*-nitrosated PLGH-cysteine films. Each data point corresponds to the average and standard deviation of $n \geq 6$.

time (h)	mmol RSNO g ⁻¹	mmol NO g ⁻¹
0	0.138 ± 0.012	0.000 ± 0.000
10	0.129 ± 0.011	0.012 ± 0.003
20	0.120 ± 0.009	0.027 ± 0.007
30	0.104 ± 0.022	0.033 ± 0.006

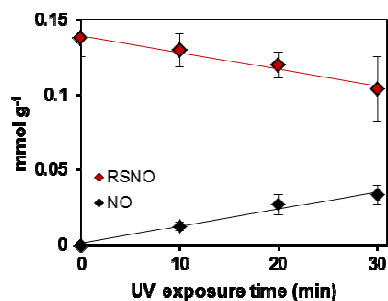


Figure 3. The RSNO decomposition (red) and NO release (black) profiles as a function of UV exposure time for *S*-nitrosated PLGH-cysteine films under dry, deoxygenated conditions. Each data point corresponds to the average and standard deviation of $n \geq 6$.

The overall NO yields are highly dependent on the decomposition pathway employed. In particular, UV irradiation had demonstrated a significant increase in NO release rates for *S*-nitrosated materials compared to thermal conditions.^{7,9,10} The RSNO soaking studies performed, displayed in Figure 2, show a smaller amount of NO release over a longer time period, while the UV irradiation studies, displayed in Figure 3, give rise to a larger amount of NO release in a shorter amount of time. Although the release rates are quite variable among decomposition pathways, the correlation

between the RSNO decomposition and NO recovery can be analyzed regardless.

Conclusions

Overall, the % NO recovery and % RSNO decomposition values match at each time point under various deoxygenated conditions, demonstrating that the RSNO is the predominant source of NO release in the system. More specifically, RSNO decomposition correlated to NO release for *S*-nitrosated PLGH-cysteine films exposed to buffer at 37 °C as well as films exposed to UV light under dry, ambient temperature conditions. The conditions reported herein are relevant to RSNO applications, where the decomposition is initiated primarily through thermal, pH and UV triggered stimuli.³ More specifically, the experimental conditions of buffer soak at 37 °C enable pH and thermal initiated decomposition, while the dry, UV conditions enable UV initiated decomposition of the RSNO. While these studies were performed under the deoxygenated conditions required for the NOA standard setup, the spectroscopic methods described herein can be applied to compare donor behavior and NO release in general. More specifically, a validated NO measurement technique capable of sensitive NO detection under oxygenated conditions could be coupled to spectroscopic analysis of the donor to understand material behavior and therapeutic delivery for bioapplications. This study marks the first time that the RSNO decomposition has been directly correlated to NO release for a polymer system, thereby implicating the *S*-nitrosothiol moiety as the predominant source of NO. Most studies simply assume that the RSNO moiety gives rise to NO, while this process is not directly probed. Since there can be alternate sources of NO in the system, such as residual nitrosating agent or other nitroso products, it is necessary to directly measure the RSNO behaviour to ensure that the RSNO decomposition correlates directly to NO release.

It should be noted that this study has been performed using a model polymer system with a corresponding solvent that is appropriate to solubilize the polymer while not destabilizing the RSNO, thus making it appropriate for solution-phase UV-vis analysis. However, there are many polymers that are not readily soluble, therefore making them inappropriate for solution-phase UV-vis. In such a case, solid state UV-vis measurements, such as diffuse reflectance, can be employed. In addition, a polymer that does not absorb in the 300-400 nm wavelength region is required to monitor the absorbance feature at 335 nm due to the $n_o \rightarrow \pi^*$ transition. To analyze RSNO content for a polymer with interference in this region, it is possible to instead monitor the 550-600 nm band that is due to the $n_N \rightarrow \pi^*$ transition.³ Since the 550-600 nm absorbance feature exhibits a significantly smaller ϵ_{max} value (~ 20 M⁻¹ cm⁻¹ compared to $\sim 10^3$ M⁻¹ cm⁻¹), a higher concentration of polymer would be required for this analysis to increase the concentration of RSNO in solution to a detectable level. However, the extinction coefficient for the 300-400 nm absorbance feature is roughly 50× that of the coefficient for the 550-600 nm feature. Since a 3.5 mg mL⁻¹ polymer solution was required to yield an absorbance value of ~ 0.1 for analysis at 335 nm, analysis at ~ 550 nm would require a polymer solution on the order of >100 mg mL⁻¹ which could be beyond the solubility range of the polymer. Thus, analysis at 550 nm of the RSNO is limited by the solubility of the polymer in question.

The ability to correlate NO release with RSNO decomposition is important for confirming that the RSNO in the polymer is responsible for the NO release. These methods

are intended to be applied, not just to the model PLGH system described here, but to all NO releasing materials (both biodegradable and biostable). This will ensure that each unique system is yielding NO from the intended source, rather than potential byproducts or residual species present in the system. The ability to confirm that the NO reservoirs within materials are predominantly due to the donor of interest will enable understanding of the NO material behaviour for subsequent application. Once the fundamental physical processes occurring within NO releasing films are completely understood, these materials can be further applied in biomedical settings.

Acknowledgements

We would like to acknowledge Colorado State University and the Department of Defense Congressionally Directed Medical Research Program (DOD-CDMPRP) for financial support. This research was supported by funds from the Boettcher Foundation's Webb-Waring Biomedical Research Program. We would like to further acknowledge Dr. Vinod Damodaran for providing the PLGH-cysteine material for these studies.

Notes and references

^a Department of Chemistry, Colorado State University, 1872 Campus Delivery, Fort Collins, CO 80523.

^b School of Biomedical Engineering, 1872 Campus Delivery, Colorado State University, Fort Collins, CO 80523.

- M. C. Frost, M. M. Reynolds and M. E. Meyerhoff, *Biomaterials*, 2005, **26**, 1685; V. N. Varu, N. D. Tsihlis and M. R. Kibbe, *Vasc. Endovascular Surg.*, 2009, **43**, 121; A. B. Seabra and N. Duran, *J. Mater. Chem.*, 2010, **20**, 1624; D. A. Riccio and M. H. Schoenfisch, *Chem. Soc. Rev.*, 2012, **41**, 3731; M. C. Jen, M. C. Serrano, R. van Lith and G. A. Ameer, *Adv. Funct. Mater.*, 2012, **22**, 239.
- J. A. Hrabie and L. K. Keefer, *Chem. Rev.*, 2002, **102**, 1135.
- D. L. H. Williams, *Acc. Chem. Res.*, 1999, **32**, 869.
- W. R. Mathews and S. W. Kerr, *J. Pharmacol. Exp. Ther.*, 1993, **267**, 1529; J. S. Stamler, D. I. Simon, J. A. Osborne, M. E. Mullins, O. Jaraki, T. Michel, D. J. Singel and J. Loscalzo, *Proc. Natl. Acad. Sci. USA*, 1992, **89**, 444.
- M. C. Frost, M. E. Meyerhoff, *J. Am. Chem. Soc.*, 2004, **126**, 1348; D. A. Riccio, J. L. Nugent and M. H. Schoenfisch, *Chem. Mater.*, 2011, **23**, 1727; N. A. Stasko, T. H. Fischer and M. H. Schoenfisch, *Biomacromolecules*, 2008, **9**, 834.
- A. B. Seabra, R. da Silva, M. G. de Oliveira, *Biomacromolecules*, 2005, **6**, 2512; P. N. Coneski, K. S. Rao, M. H. Schoenfisch, *Biomacromolecules*, 2010, **11**, 3208.
- P. N. Coneski, M. H. Schoenfisch, *Polym. Chem.*, 2011, **2**, 906.
- K. S. Bohl, J. L. West, *Biomaterials*, 2000, **21**, 2273; E. A. Lipke, J. L. West, *Acta Biomater.*, 2005, **1**, 597.
- N. A. Stasko, T. H. Fischer, M. H. Schoenfisch, *Biomacromolecules*, 2008, **9**, 834.
- D. A. Riccio, K. P. Dobmeier, E. M. Hetrick, B. J. Privett, H. S. Paul, M. H. Schoenfisch, *Biomaterials*, 2009, **30**, 4494
- D. A. Riccio, P. N. Coneski, S. P. Nichols, A. D. Broadnax, M. H. Schoenfisch, *ACS Appl. Mater. Interfaces*, 2012, **4**, 796.
- A. B. Seabra, R. da Silva, G. F. P. de Souza, M. G. de Oliveira, *Artif. Organs*, 2008, **32**, 262; Y. Li, P. I. Lee, *Mol. Pharmaceutics*, 2010, **7**, 254.
- D. J. Barnett, J. McAninly, D. L. H. Williams, *J. Chem. Soc. Perkin Trans. 2*, 1994, 1131.
- D. L. H. Williams, *Nitrosation Reactions and the Chemistry of Nitric Oxide*. Elsevier: 2004.
- J. M. Joslin and M. M. Reynolds, *ACS Appl. Mater. Interfaces*, 2012, **4**, 1126.
- M. Feelisch, J. S. Stamler, *Methods in Nitric Oxide Research*. John Wiley & Sons Ltd: 1996.
- J. M. Joslin, V. B. Damodaran and M. M. Reynolds, *RSC Adv.*, 2013, **3**, 15035.
- M. C. Frost and M. E. Meyerhoff, *J. Biomed. Mater. Res., Part A*, 2005, **72A**, 409; T. A. Johnson, N. A. Stasko, J. L. Matthews, W. E. Cascio, E. L. Holmuhamedov, C. B. Johnson and M. H. Schoenfisch, *Nitric Oxide*, 2010, **22**, 30
- Y. Li and P. I. Lee, *Mol. Pharmaceutics*, 2010, **7**, 254.
- V. B. Damodaran, J. M. Joslin, K. A. Wold, S. M. Lantvit and M. M. Reynolds, *J. Mater. Chem.*, 2012, **22**, 5990.
- L. Grossi and P. C. Montevecchi, *Chem. Eur. J.*, 2002, **8**, 380.
- R. J. Singh, N. Hogg, J. Joseph and B. Kalyanaraman, *J. Biol. Chem.*, 1996, **271**, 18596; V. R. Zhelyaskov, K. R. Gee and D. W. Godwin, *Photochem. Photobiol.*, 1998, **67**, 282; P. D. Wood, B. Mutus and R. W. Redmond, *Photochem. Photobiol.*, 1996, **64**, 518; D. J. Sexton, A. Muruganandam, D. J. McKenney and B. Mutus, *Photochem. Photobiol.*, 1994, **59**, 463.

COMMUNICATION

Table of contents entry for “Correlating S-nitrosothiol decomposition and NO release for modified poly(lactic-co-glycolic acid) polymer films”
by J. M. Joslin, B. H. Neufeld, and M. M. Reynolds

The decomposition of an *S*-nitrosated model polymer was correlated to the subsequent release of nitric oxide under multiple decomposition pathways.

